Preface

Precision studies of simple atomic and molecular systems are a multidisciplinary field in modern physics. They massively involve methods and objects from very different areas of physics.

Experimental methods vary from laser spectroscopy to accelerator physics, from laboratory desktop-scale experiments to space missions. On the theoretical side they deal with methods of molecular, atomic, nuclear, and particle physics.

The specific feature of this area is that the simple atoms and molecules are not the object of the studies, but a powerful instrument to look into the deepest and most basic problems of physics. The most advanced precision measurements allow us to see various tiny effects, while the atomic simplicity provides us with the possibility of keeping the atomic details under control and looking into a substantially more fundamental level.

Simple atoms and molecules provide us with a good opportunity to measure fundamental constants, to look for possible violation of basic symmetries, to study properties of elementary particles and nuclei.

This book is based on extended review lectures from two recent international meetings on simple atoms and presents the most recent progress in the field. I am grateful to Claudio Lenz Cesar, Jochen Walz, and Theodor W. Hänsch, who were co-organizers of these meetings (Mangaratiba, 2004, and Venice, 2006) and made great efforts to make these meetings happen, and to many other colleagues, whose help in organizing the meetings was important.

St.Petersburg—Garching *Savely Karshenboim*
April, 2007

Part I

Precision Measurements and Fundamental Constants

The Muon $g-2$: Status and Perspectives

F. Jegerlehner

Humboldt-Universität zu Berlin, Institut für Physik, Newtonstrasse 15, D-12489 Berlin, Germany and DESY, Platanenallee 6, D-15738 Zeuthen, Germany
fjeger@physik.hu-berlin.de

Abstract. The muon anomalous magnetic moment is one of the most precisely measured quantities in particle physics. Recent high-precision measurements (0.5 ppm) at Brookhaven reveal a "discrepancy" by three standard deviations from the electroweak Standard Model which could be a hint for an unknown contribution from physics beyond the Standard Model. This triggered numerous speculations about the possible origin of the "missing piece". The remarkable 15-fold improvement of the previous CERN experiment actually animated a multitude of new theoretical efforts which led to a substantial improvement of the prediction of a_μ. The dominating uncertainty of the prediction, caused by strong interaction effects, could be reduced substantially, due to new hadronic cross-section measurements in electron–positron annihilation at low energies. After an introduction and a brief description of the principle of the experiment, I review the status of the theoretical prediction and discuss the role of the hadronic vacuum polarization effects and the hadronic light-by-light scattering contribution. Prospects for the future will be briefly discussed. As, in electroweak precision physics, the muon $g-2$ shows the largest established deviation between theory and experiment at present, it will remain one of the hot topics in future also.

1 Lepton Magnetic Moments

The subject of our interest is the motion of a lepton in an external electromagnetic field under consideration of the full relativistic quantum behavior. The latter is controlled by the equations of motion of quantum electrodynamics (QED), which describes the interaction of charged leptons ($\ell = \mathrm{e}, \mu, \tau$) with the photon ($\gamma$) as an Abelian $U(1)_{\mathrm{em}}$ gauge theory. QED is a quantum field theory (QFT) which emerges as a synthesis of quantum mechanics with special relativity. In our case an external electromagnetic field is added, specifically a constant homogeneous magnetic field $\mathbf{B}$. For slowly varying fields the motion is essentially determined by the generalized Pauli equation, which also serves as a basis for understanding the role of the magnetic moment of a lepton on the classical level. As we will see below, in the absence of electrical fields $\mathbf{E}$ the

F. Jegerlehner: *The Muon $g-2$: Status and Perspectives*, Lect. Notes Phys. **745**, 9–34 (2008)
DOI 10.1007/978-3-540-75479-4_2 © Springer-Verlag Berlin Heidelberg 2008

quantum correction miraculously may be subsumed in a single number, the anomalous magnetic moment a_ℓ, which is the result of relativistic quantum fluctuations, usually simply called *radiative corrections*.

Charged leptons in the first place interact with photons, and photonic radiative corrections can be calculated in QED, the interaction Lagrangian density of which is given by (e the magnitude of the electron's charge)

$$\mathcal{L}_{\rm int}^{\rm QED}(x) = e j^\mu_{\rm em}(x)\, A_\mu(x) \;\;,\;\; j^\mu_{\rm em}(x) = -\sum_\ell \bar\psi_\ell(x)\gamma^\mu\psi_\ell(x)\;, \tag{1}$$

where $j^\mu_{\rm em}(x)$ is the electromagnetic current, $\psi_\ell(x)$ the Dirac field describing the lepton ℓ, γ^μ the Dirac matrices and with a photon field $A_\mu(x)$ exhibiting an external classical component $A^{\rm ext}_\mu$ and hence $A_\mu \to A_\mu + A^{\rm ext}_\mu$. We are thus dealing with QED exhibiting an additional external field insertion "vertex".

Besides charge, spin, mass and lifetime, leptons have other very interesting static (classical) electromagnetic and weak properties like the magnetic and electric dipole moments. A well-known example is the circulating current, due to an orbiting particle with electric charge e and mass m, which exhibits a magnetic dipole moment $\boldsymbol{\mu}_L = \frac{1}{2c} e\, \mathbf{r}\times\mathbf{v}$ given by

$$\boldsymbol{\mu}_L = \frac{e}{2mc}\,\mathbf{L} \tag{2}$$

where $\mathbf{L} = m\,\mathbf{r}\times\mathbf{v}$ is the orbital angular momentum ($\mathbf{r}$ position, $\mathbf{v}$ velocity). As we know, leptons have spin (intrinsic angular momentum) $\frac{1}{2}$, which is directly responsible for the intrinsic magnetic moment. The fundamental relation which defines the "g-factor" or the magnetic moment is

$$\boldsymbol{\mu} = g_\ell\,\frac{e\hbar}{2m_\ell c}\,\mathbf{s}\;,\;\; \mathbf{s}\;\text{ the spin vector.} \tag{3}$$

For leptons, the Dirac theory predicts $g_\ell = 2$ [1], unexpectedly, twice the value $g = 1$ known to be associated with orbital angular momentum. It took about 20 years of experimental efforts to establish that the electrons' magnetic moment actually exceeds 2 by about 0.12%, the first clear indication of the existence of an "anomalous" contribution to the magnetic moment [2]. In general, the anomalous magnetic moment of a lepton is related to the gyromagnetic ratio by

$$a_\ell = \mu_\ell/\mu_{\rm B} - 1 = \frac{1}{2}(g_\ell - 2)\;,\;\; (\ell = {\rm e}, \mu, \tau), \tag{4}$$

where $\mu_{\rm B}$ is the Bohr magneton.

Formally, the anomalous magnetic moment is given by a form factor, defined by the matrix element

$$\langle \ell^-(p')|j^\mu_{\rm em}(0)|\ell^-(p)\rangle$$

where $|\ell^-(p)\rangle$ is a lepton state of momentum p. The relativistically covariant decomposition of the matrix element reads

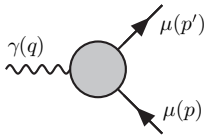

$$= (-\mathrm{i}e)\, \bar{u}(p') \left[\gamma^\mu F_\mathrm{E}(q^2) + \mathrm{i}\tfrac{\sigma^{\mu\nu} q_\nu}{2m_\mu} F_\mathrm{M}(q^2)\right] u(p)$$

with $q = p' - p$ and where $u(p)$ denotes a Dirac spinor, the relativistic wave function of a free lepton, a classical solution of the Dirac equation $(\gamma^\mu p_\mu - m)\, u(p) = 0$. $F_\mathrm{E}(q^2)$ is the electric charge or Dirac form factor and $F_\mathrm{M}(q^2)$ is the magnetic or Pauli form factor. Note that the matrix $\sigma^{\mu\nu} = \frac{\mathrm{i}}{2}[\gamma^\mu, \gamma^\nu]$ represents the spin 1/2 angular momentum tensor. In the static (classical) limit $q^2 \to 0$ we have

$$F_\mathrm{E}(0) = 1 \;\; ; \quad F_\mathrm{M}(0) = a_\mu \tag{5}$$

where the first relation is the charge normalization condition, which must be satisfied by the electrical form factor, while the second relation defines the anomalous magnetic moment. a_μ is a finite prediction in any renormalizable QFT: QED, the Standard Model (SM) or any renormalizable extension of it.

By the end of the 1940s the breakthrough in understanding and handling renormalization of QED had made unambiguous predictions of higher order effects possible, and in particular of the leading (one-loop diagram) contribution to the anomalous magnetic moment

$$a_\ell^{\mathrm{QED}(1)} = \frac{\alpha}{2\pi}\,, (\ell = \mathrm{e}, \mu, \tau) \tag{6}$$

by Schwinger in 1948 [3]. This contribution is due to quantum fluctuations via virtual photon–lepton interactions and in QED is universal for all leptons. At higher orders, in the perturbative expansion, other effects come into play: strong interaction, weak interaction, both included in the SM, as well as yet unknown physics which would contribute to the anomalous magnetic moment.

In fact, shortly before Schwinger's QED prediction, Kusch and Foley in 1948 established the existence of the electron "anomaly" $g_\mathrm{e} = 2\,(1.00119 \pm 0.00005)$, a 1.2 per mill deviation from the value 2 predicted by Dirac in 1928.

We now turn to the muon. A muon looks like a copy of an electron, which at first sight is just much heavier $m_\mu/m_\mathrm{e} \sim 200$; however, unlike the electron it is unstable and its lifetime is actually rather short. The decay proceeds by weak charged current interaction into an electron and two neutrinos.

The muon is very interesting for the following reason: quantum fluctuations due to heavier particles or contributions from higher energy scales are proportional to

$$\frac{\delta a_\ell}{a_\ell} \propto \frac{m_\ell^2}{M^2} \qquad (M \gg m_\ell)\,, \tag{7}$$

where M may be

- the mass of a heavier SM particle, or
- the mass of a hypothetical heavy state beyond the SM, or
- an energy scale or an ultraviolet cut-off where the SM ceases to be valid.

On the one hand, this means that the heavier the new state or scale the harder it is to see (it decouples as $M \to \infty$), typically the best sensitivity we have for nearby new physics, which has not yet been discovered by other experiments. On the other hand, the sensitivity to "new physics" grows quadratically with the mass of the lepton, which means that the interesting effects are magnified in a_μ relative to a_e by a factor $(m_\mu/m_e)^2 \sim 4 \times 10^4$. This is what makes the anomalous magnetic moment of the muon the predestinated "monitor for new physics" or if no deviation is found it may provide severe constraints to physics beyond the SM.

In contrast, a_e is relatively insensitive to unknown physics and can be predicted very precisely, and therefore it presently provides the most precise determination of the fine structure constant $\alpha = e^2/4\pi$.

What makes the muon so special for what concerns its anomalous magnetic moment?

- Most interesting is the enhanced high sensitivity of a_μ to all kind of interesting physics effects.
- Both experimentally and theoretically a_μ is a "clean" observable, i.e., it can be measured with high precision as well as predicted unambiguously in the SM.
- That a_μ can be measured so precisely is a kind of miracle and possible only due to the specific properties of the muon. Due to the parity violating weak (V–A) interaction property, muons can easily be polarized and perfectly transport polarization information to the electrons produced in their decay.
- There exists a magic energy ("magic γ") at which equations of motion take a particularly simple form. Miraculously, this energy is so high (3.1 GeV) that the μ lives 30 times longer than in its rest frame! In fact only these highly energetic muons can be collected in a muon storage ring. At much lower energies muons could not be stored long enough to measure the precession precisely!

Production and decay of the muons goes by the chain

$$\begin{aligned} &\pi \to \mu + \nu_\mu \\ &\qquad\quad \hookrightarrow\ e + \nu_e + \nu_\mu \end{aligned}$$

2 The BNL Muon $g-2$ Experiment

The first measurement of the anomalous magnetic moment of the muon became possible at the CERN cyclotron (1958–1962) [4] in 1961. Surprisingly, nothing special was observed within the 0.4% level of accuracy of the experiment. It was the first real evidence that the muon was just a heavy electron. In particular this meant that the muon is point-like and no extra short distance

effects could be seen. This latter point of course is a matter of accuracy and the challenge to go further was evident.

The idea of a muon storage ring was put forward next. A first one was successfully realized at CERN (1962–1968) [5]. It allowed to measure a_μ for both μ^+ and μ^- at the same machine. Results agreed well within errors and provided a precise verification of the CPT theorem for muons. An accuracy of 270 ppm was reached and an insignificant 1.7 σ ($1\sigma = 1$ standard deviation) deviation from theory was found. Nevertheless the latter triggered a reconsideration of theory. It turned out that in the estimate of the three-loop $O(\alpha^3)$ QED contribution the leptonic light-by-light scattering part (dominated by the electron loop) was missing. Aldins et al. [6] then calculated this and after including it, perfect agreement between theory and experiment was obtained.

The CERN muon $g-2$ experiment was shut down at the end of 1976, while data analysis continued to 1979 [7]. Only a few years later, in 1984 the E821collaboration formed, with the aim to perform a new experiment at Brookhaven National Laboratory (BNL). Data taking was between 1998 and 2001. Data analysis was completed in 2004. The E821 $g-2$ measurements achieved the remarkable precision of 0.5 ppm [8], which is a 15-fold improvement of the CERN result. The principle of the BNL muon $g-2$ experiments involves the study of the orbital and spin motion of highly polarized muons in a magnetic storage ring. This method has been applied in the last CERN experiment already. The key improvements of the BLN experiment include the very high intensity of the primary proton beam from the alternating gradient synchrotron (AGS), the injection of muons instead of pions into the storage ring and a superferric storage ring magnet. The protons hit a target and produce pions. The pions are unstable and decay into muons plus a neutrino where the muons carry spin and thus a magnetic moment which is directed along the direction of the flight axis. The longitudinally polarized muons from pion decay are then injected into a uniform magnetic field $\mathbf{B}$ where they travel in a circle. If one lets travel polarized muons on a circular orbit in a constant magnetic field, as illustrated in Fig. 1, then a_μ is responsible for the Larmor precession of the direction of the spin of the muon, characterized by the angular frequency $\boldsymbol{\omega}_\mathrm{a}$. At the magic energy of about ~ 3.1 GeV, the latter is directly proportional to a_μ:

$$\boldsymbol{\omega}_\mathrm{a} = \frac{e}{m}\left[a_\mu \mathbf{B} - \left(a_\mu - \frac{1}{\gamma^2-1}\right)\boldsymbol{\beta}\times\mathbf{E}\right]_{\text{at “magic }\gamma\text{”}}^{E\sim 3.1\,\mathrm{GeV}} \simeq \frac{e}{m}\left[a_\mu \mathbf{B}\right]. \qquad (8)$$

Electric quadrupole fields $\mathbf{E}$ are needed for focusing the beam and they affect the precession frequency in general. $\gamma = E/m_\mu = 1/\sqrt{1-\beta^2}$ is the relativistic Lorentz factor with $\beta = v/c$, the velocity of the muon in units of the speed of light c. The magic energy $E_\mathrm{mag} = \gamma_\mathrm{mag} m_\mu$ is the energy E for which $\frac{1}{\gamma_\mathrm{mag}^2-1} = a_\mu$. The existence of a solution is due to the fact that a_μ is a positive constant in competition with an energy-dependent factor of opposite sign (as $\gamma \geq 1$). The second miracle, which is crucial for the feasibility of the

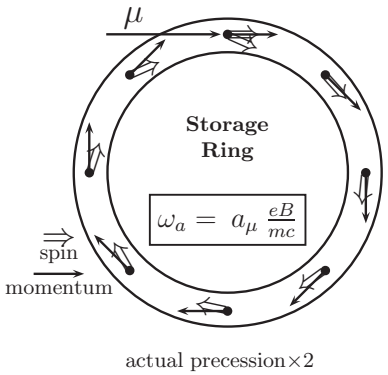

Fig. 1. Spin precession in the $g-2$ ring ($\sim 12°$/circle)

experiment, is the fact that $\gamma_{\rm mag} = \sqrt{(1+a_\mu)/a_\mu} \simeq 29.378$ is large enough to provide the time dilatation factor for the unstable muon boosting the life time $\tau_\mu \simeq 2.197 \times 10^{-6}$ s to $\tau_{\rm in\,flight} = \gamma\,\tau_\mu \simeq 6.454 \times 10^{-5}$ s, which allows the muons, traveling at $v/c = 0.99942\ldots$, to be stored in a ring of reasonable size (diameter $\sim$ 14 m). This provided the basic setup for the $g-2$ experiments at the muon storage rings at CERN and BNL. The oscillation frequency $\boldsymbol{\omega}_{\rm a}$ can be measured very precisely. Also the precise tuning to the magic energy is not the major problem. The most serious challenge is to manufacture a precisely known constant magnetic field B, as the latter directly enters the experimental extraction of a_μ (8). Of course one also needs high-enough statistics to get sharp values for the oscillation frequency. The basic principle of the measurement of a_μ is a measurement of the "anomalous" frequency difference $\omega_{\rm a} = |\boldsymbol{\omega}_{\rm a}| = \omega_{\rm s} - \omega_{\rm c}$, where $\omega_{\rm s} = g_\mu\,(e\hbar/2m_\mu)\,B/\hbar = g_\mu/2 \cdot e/m_\mu B$ is the muon spin–flip precession frequency in the applied magnetic field and $\omega_{\rm c} = e/m_\mu\ B$ is the muon cyclotron frequency. Instead of eliminating the magnetic field by measuring $\omega_{\rm c}$, B is determined from proton nuclear magnetic resonance (NMR) measurements. This procedure requires the value of $\mu_\mu/\mu_{\rm p}$ to extract a_μ from the data. Fortunately, a high-precision value for this ratio is available from the measurement of the hyperfine structure in muonium. One obtains

$$a_\mu = \frac{\bar{R}}{|\mu_\mu/\mu_{\rm p}| - \bar{R}}\ , \tag{9}$$

where $\bar{R} = \omega_{\rm a}/\bar{\omega}_{\rm p}$ and $\bar{\omega}_{\rm p} = (e/m_\mu c) < B >$ is the free proton NMR frequency which corresponds to the average magnetic field, seen by the muons in their orbits in the storage ring. We mention that for the electron a Penning trap is employed to measure $a_{\rm e}$ rather than a storage ring. The B field in this case can be eliminated via a measurement of the cyclotron frequency.

Since the spin precession frequency can be measured very well, the precision at which $g-2$ can be measured is essentially determined by the possibility

to manufacture a constant homogeneous magnetic field $\mathbf{B}$. Important but easier to achieve is the tuning to the magic energy.

3 Standard Model Prediction for a_μ

The anomalous magnetic moment a_ℓ is a dimensionless quantity, just a number, and corresponds to an effective tensor interaction term

$$\delta\mathcal{L}_{\rm eff}^{\rm AMM} = -\frac{e_\ell a_\ell}{4m_\ell}\,\bar\psi(x)\,\sigma^{\mu\nu}\,\psi(x)\,F_{\mu\nu}(x)\ , \tag{10}$$

which in an external magnetic field at low energy takes the well-known form of a magnetic energy (up to a sign)

$$\delta\mathcal{L}_{\rm eff}^{\rm AMM} = -\mathcal{H}_{\rm m} \simeq -\frac{e_\ell a_\ell}{2m_\ell}\,\boldsymbol{\sigma}\mathbf{B}\ . \tag{11}$$

Such a term, if present in the fundamental Lagrangian, would spoil renormalizability of the theory and contribute to $F_{\rm M}(q^2)$ at the tree level. In addition, it is not $SU(2)_L$ gauge invariant, because gauge invariance only allows minimal couplings via a covariant derivative, i.e., vector and/or axial-vector terms. The emergence of an anomalous magnetic moment term in the SM is a consequence of the symmetry breaking by the Higgs mechanism, which provides the mass to the physical particles and allows for helicity flip processes like the anomalous magnetic moment transitions. In any renormalizable theory the anomalous magnetic moment term must vanish at tree level. This means that there is no free adjustable parameter associated with it. Actually, it is a finite prediction of the theory.

The reason why it is so interesting to have such a precise measurement of $a_{\rm e}$ or a_μ of course is that it can be calculated with comparable accuracy in theory by a perturbative expansion in α of the form

$$a_\ell \simeq \sum_{n=1}^{N} A^{(2n)}(\alpha/\pi)^n\ , \tag{12}$$

with up to $N = 5$ terms under consideration at present. The recent new determination of $a_{\rm e}$ [9] allows for a very precise determination of the fine structure constant [10]:

$$\alpha^{-1}(a_{\rm e}) = 137.035999070(98)\,[0.71\,{\rm ppb}]\ , \tag{13}$$

which we will use for the evaluation of a_μ.

At two and more loops results depend on lepton mass ratios. For the evaluation of these contributions precise values for the lepton masses are needed. We will use the following values for the muon–electron mass ratio, the muon and the tau mass [11, 12]:

$$\begin{gathered} m_\mu/m_{\rm e} = 206.768\,2838\,(54)\ ,\quad m_\mu/m_\tau = 0.059\,4592\,(97) \\ m_{\rm e} = 0.510\,9989\,918(44)\ {\rm MeV}\ ,\quad m_\mu = 105.658\,3692\,(94)\ {\rm MeV} \\ m_\tau = 1776.99\,(29)\ {\rm MeV}\ . \end{gathered} \tag{14}$$

3.1 The Universal QED Contribution

The leading contributions to a_ℓ can be calculated in QED. With increasing precision, higher and higher terms become relevant. At present, 4 loops are indispensable and strong interaction effects like hadronic vacuum polarization (vap) or hadronic light-by-light scattering (lbl) as well as weak effects have to be considered. Typically, analytic results for higher order terms may be expressed in terms of the Riemann zeta function:

$$\zeta(n) = \sum_{k=1}^{\infty} \frac{1}{k^n} \tag{15}$$

and of the poly-logarithmic integrals

$$\mathrm{Li}_n(x) = \frac{(-1)^{n-1}}{(n-2)!} \int_0^1 \frac{\ln^{n-2}(t)\ln(1-tx)}{t} \mathrm{d}t = \sum_{k=1}^{\infty} \frac{x^k}{k^n} \ . \tag{16}$$

We first discuss the universal contributions a_ℓ where internal and external leptons are of the same type ℓ (one flavor QED): at leading order one has

• One 1-loop diagram

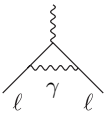

$$a_{\mathrm{e}} = a_\mu = a_\tau = \tfrac{\alpha}{2\pi}$$

Schwinger 1948 [3] giving the result mentioned before.

• At 2-loops seven diagrams with one type of fermion lines

which contribute a term

$$a_\ell^{(4)} = \left[\frac{197}{144} + \frac{\pi^2}{12} - \frac{\pi^2}{2}\ln 2 + \frac{3}{4}\zeta(3)\right] \left(\frac{\alpha}{\pi}\right)^2 \ , \tag{17}$$

obtained independently by Petermann [13] and Sommerfield [14] in 1957.

• At 3-loops, with ℓ-type fermion lines only, 72 diagrams contribute. Most remarkably, after about 25 years of hard work, Laporta and Remiddi in 1996 [15] managed to give a complete analytic result:

$$a_\ell^{(6)} = \left[\frac{28259}{5184} + \frac{17101}{810}\pi^2 - \frac{298}{9}\pi^2\ln 2 + \frac{139}{18}\zeta(3) + \frac{100}{3}\left\{\mathrm{Li}_4\left(\frac{1}{2}\right) + \frac{1}{24}\ln^4 2 - \frac{1}{24}\pi^2\ln^2 2\right\} - \frac{239}{2160}\pi^4 + \frac{83}{72}\pi^2\zeta(3) - \frac{215}{24}\zeta(5)\right] \left(\frac{\alpha}{\pi}\right)^3 \ . \tag{18}$$

It was confirming Kinoshita's earlier numerical evaluation [16]. The big advantage of the analytic result is that it allows a numerical evaluation at any desired precision. The direct numerical evaluation of the multidimensional Feynman integrals by Monte Carlo methods is always of limited precision and an improvement is always very expensive in computing power.

• At 4-loops 891 diagrams contribute to the universal term. Their evaluation is possible by numerical integration and has been performed in a heroic effort by Kinoshita [17] (reviewed in [18]) and was updated recently by Kinoshita and collaborators (2006/2007) [19, 20].

The largest uncertainty comes from 518 diagrams without fermion-loops contributing to the universal term $A_1^{(8)}$. Completely unknown is the universal 5-loop term $A_1^{(10)}$, which is leading for a_{e}. Some estimation discussed in [21] suggests an uncertainty of 3.8 for the 5-loop coefficient. We adopt this estimate and take into account $A_1^{(10)} = 0.0(3.8)$ (as in [19]).

Collecting the universal terms we have

$$\begin{aligned} a_\ell^{\mathrm{uni}} &= 0.5\left(\frac{\alpha}{\pi}\right) - 0.32847896557919378\ldots\left(\frac{\alpha}{\pi}\right)^2 \\ &\quad +1.181241456587\ldots\left(\frac{\alpha}{\pi}\right)^3 - 1.7283(35)\left(\frac{\alpha}{\pi}\right)^4 + 0.0(3.8)\left(\frac{\alpha}{\pi}\right)^5 \\ &= 0.001\,159\,652\,176\,42(81)(10)(26)\,[86]\ldots \end{aligned} \tag{19}$$

for the one-flavor QED contribution. The three errors are: the error of α, given in (13), the numerical uncertainty of the α^4 coefficient and the estimated size of the missing higher order terms, respectively.

3.2 Mass-Dependent QED Contribution

At two loops and higher, internal fermion-loops show up, where the flavor of the internal fermion differs from the one of the external lepton, in general. As all fermions have different masses, the fermion-loops give rise to mass-dependent effects, which were calculated at 2-loops in [22, 23] (see also [24, 25, 26]), and at 3-loops in [27, 28, 29, 30, 31, 32]. The leading mass-dependent effects come from photon vacuum polarization, which leads to charge screening manifest in the "running" of α. The corresponding shift in the fine structure constant comes from the leptons (lep = e, μ and τ), the five light quarks (u, b, s, c and b) and/or the corresponding hadrons (had). The running of α is governed by the renormalization group (RG).

Typical contributions are the following:

- LIGHT internal masses give rise to logs of mass ratios which become singular in the light mass to zero limit (logarithmically enhanced corrections):

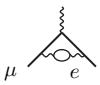

$$= \left[\tfrac{1}{3}\ln\frac{m_\mu}{m_e} - \tfrac{25}{36} + O\left(\frac{m_e}{m_\mu}\right)\right]\left(\tfrac{\alpha}{\pi}\right)^2 .$$

- HEAVY internal masses decouple, i.e., they give no effect in the heavy mass to infinity limit:

$$= \left[\frac{1}{45}\left(\frac{m_e}{m_\mu}\right)^2 + O\left(\frac{m_e^4}{m_\mu^4}\ln\frac{m_\mu}{m_e}\right)\right]\left(\frac{\alpha}{\pi}\right)^2 .$$

New physics contributions from states which are too heavy to be produced at present accelerator energies typically give this kind of contribution. Even though a_μ is 786 times less precise than a_e it is still 54 times more sensitive to new physics (NP).

Corrections due to internal e, μ- and τ-loops are different for a_e,[1] a_μ and a_τ.

The SM prediction of a_μ looks formally very similar to the one for a_e; however, besides the common universal part, the mass-dependent, the hadronic and the weak effects enter with very different weight and significance. The mass-dependent QED corrections follow from the universal set of diagrams by replacing the closed internal μ-loops by e- and/or τ-loops. Typical contributions come from vacuum polarization or light-by-light scattering loops, like

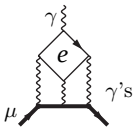

$$a_\mu^{(6)}(\mathrm{lbl}, e) = \left[\frac{2}{3}\pi^2\ln\frac{m_\mu}{m_e} + \frac{59}{270}\pi^4 - 3\,\zeta(3) - \frac{10}{3}\pi^2 + \frac{2}{3} + O\left(\frac{m_e}{m_\mu}\ln\frac{m_\mu}{m_e}\right)\right]\left(\frac{\alpha}{\pi}\right)^3 .$$

The result is given by

$$a_\mu = a_e^{\mathrm{uni}} + a_\mu(m_\mu/m_e) + a_\mu(m_\mu/m_\tau) + a_\mu(m_\mu/m_e, m_\mu/m_\tau) \tag{22}$$

with [23, 30, 31, 32]

[1] A new extraordinary precise value

$$a_e^{\mathrm{exp}} = 0.001\,159\,652\,180\,85(76) \tag{20}$$

for a_e has been obtained recently [9]. By comparison with the theoretical result $\alpha(a_e)$ (13) has been obtained. The result is of the form $a_e^{\mathrm{QED}} = a_e^{\mathrm{uni}} + a_e(\mu) + a_e(\tau) + e_e(\mu,\tau)$ with $a_e(\mu) = 5.197\,386\,70(27) \times 10^{-7}\left(\frac{\alpha}{\pi}\right)^2 - 7.373\,941\,64(29) \times 10^{-6}\left(\frac{\alpha}{\pi}\right)^3$, $a_e(\tau) = 1.83763(60)\times 10^{-9}\left(\frac{\alpha}{\pi}\right)^2 - 6.5819(19)\times 10^{-8}\left(\frac{\alpha}{\pi}\right)^3$ and $a_e(\mu,\tau) = 0.190945(62) \times 10^{-12}\left(\frac{\alpha}{\pi}\right)^3$ [23, 30, 31]. The QED part thus may be summarized in the prediction

$$a_e^{\mathrm{QED}} = \frac{\alpha}{2\pi} - 0.328\,478\,444\,002\,90(60)\left(\frac{\alpha}{\pi}\right)^2 + 1.181\,234\,016\,828(19)\left(\frac{\alpha}{\pi}\right)^3 - 1.9144(35)\left(\frac{\alpha}{\pi}\right)^4 + 0.0(3.8)\left(\frac{\alpha}{\pi}\right)^5 + 1.706(30)\times 10^{-12} . \tag{21}$$

The last term includes the small hadronic and weak contributions: $a_e^{\mathrm{had}} = 1.67(3)\times 10^{-12}$ and $a_e^{\mathrm{weak}} = 0.036\times 10^{-12}$, respectively. Therefore a_e is almost a pure QED object and therefore an excellent observable for extracting α_{QED} based on the SM prediction.

$$
\begin{aligned}
a_\mu(m_\mu/m_e) &= 1.094\ 258\ 311\ 1\ (84)\left(\frac{\alpha}{\pi}\right)^2 + 22.868\ 380\ 02\ (20)\ \left(\frac{\alpha}{\pi}\right)^3 \\
&\quad +132.682\ 3\ (72)\left(\frac{\alpha}{\pi}\right)^4, \\
a_\mu(m_\mu/m_\tau) &= 7.8064\ (25)\times 10^{-5}\ \left(\frac{\alpha}{\pi}\right)^2 + 36.051\ (21)\times 10^{-5}\left(\frac{\alpha}{\pi}\right)^3 \\
&\quad +0.005\ (3)\left(\frac{\alpha}{\pi}\right)^4, \\
a_\mu(m_\mu/m_e, m_\mu/m_\tau) &= 52.766\ (17)\times 10^{-5}\left(\frac{\alpha}{\pi}\right)^3 + 0.037\ 594\ (83)\left(\frac{\alpha}{\pi}\right)^4;
\end{aligned}
$$

except for the last term, which has been worked out as a series expansion in the mass ratios [33, 34], all contributions are known analytically in exact form [30, 31][2] up to 3 loops. At 4 loops only a few terms are known analytically [36]. Again the relevant 4-loop contributions have been evaluated by numerical integration methods by Kinoshita and Nio [37]. The 5-loop term has been estimated to be $A_2^{(10)}(m_\mu/m_e) = 663(20)$ in [38, 39, 40].

Our knowledge of the QED result for a_μ may be summarized by

$$
\begin{aligned}
a_\mu^{\rm QED} &= \frac{\alpha}{2\pi} + 0.765\,857\,410(26)\left(\frac{\alpha}{\pi}\right)^2 \\
&+24.050\,509\,65(46)\left(\frac{\alpha}{\pi}\right)^3 + 130.8105(85)\left(\frac{\alpha}{\pi}\right)^4 + 663(20)\left(\frac{\alpha}{\pi}\right)^5. \qquad (23)
\end{aligned}
$$

We thus arrive at a QED prediction of a_μ given by

$$
a_\mu^{\rm QED} = 116\,584\,718.113(.082)(.014)(.025)(.137)[.162]\times 10^{-11} \qquad (24)
$$

where the first error is the uncertainty of α in (13), the second one combines in quadrature the uncertainties due to the errors in the mass ratios, the third is due to the numerical uncertainty and the last stands for the missing $O(\alpha^5)$ terms. With the new value of $\alpha[a_e]$ the combined error is dominated by our limited knowledge of the 5-loop term.

3.3 Weak Contributions

The electroweak SM is a non-Abelian gauge theory with gauge group $SU(2)_L\otimes U(1)_Y \to U(1)_{\rm QED}$, which is broken down to the electromagnetic Abelian subgroup $U(1)_{\rm QED}$ by the Higgs mechanism, which requires a scalar Higgs field H which receives a vacuum expectation value v. The latter fixes the experimentally well-known Fermi constant $G_\mu = 1/(\sqrt{2}v^2)$ and induces the masses of the heavy gauge bosons $M_{\rm W}$ and $M_{\rm Z}$[3] as well as all fermion masses

[2] Explicitly, the papers only present expansions in the mass ratios; some result have been extended in [32] and cross-checked against the full analytic result in [35].

[3] $M_{\rm Z} = 91.1876 \pm 0.0021$ GeV , $M_{\rm W} = 80.403 \pm 0.026$ GeV, also $m_{\rm H} > 115$ GeV.

$m_{\rm f}$. Other physical constants which we will need later for evaluating the weak contributions are the Fermi constant and the weak mixing parameter:

$$G_\mu = 1.16637(1) \times 10^{-5} \quad \text{GeV}^{-2}\ , \quad \sin^2\Theta_{\rm W} = 0.2225(5)\ . \tag{25}$$

The weak interaction contributions to a_μ are due to the exchange of the heavy gauge bosons, the charged $\rm W^\pm$ and the neutral Z, which mixes with the photon via a rotation by the weak mixing angle $\Theta_{\rm W}$ and which defines the weak mixing parameter $\sin^2\Theta_{\rm W} = 1 - M_{\rm W}^2/M_{\rm Z}^2$. What is most interesting is the occurrence of the first diagram of Fig. 2, which exhibits a non-Abelian triple gauge vertex and the corresponding contribution provides a test of the Yang–Mills structure involved. It is of course not surprising that the photon couples to the charged W boson the way it is dictated by electromagnetic gauge invariance. The gauge boson contributions up to negligible terms of order $\mathrm{O}(\frac{m_\mu^2}{M_{\rm W,Z}^2})$ are given by (the Higgs contribution is negligible)

$$a_\mu^{(2)\,\rm EW} = \left[5 + (-1 + 4\,\sin^2\Theta_{\rm W})^2\right]\ \frac{\sqrt{2}G_\mu m_\mu^2}{48\pi^2} \simeq 194.82(2) \times 10^{-11}. \tag{26}$$

The error comes from the uncertainty in $\sin^2\Theta_{\rm W}$ given above.

The electroweak 2-loop corrections have to be taken into account as well. In fact triangle fermion-loops may give rise to unexpectedly large radiative corrections. The diagrams which yield the leading corrections are those including a VVA triangular fermion-loops (VVA $\neq 0$ while VVV $= 0$) associated with a Z boson exchange

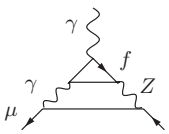

which exhibits a parity violating axial coupling (A). A fermion of flavor f yields a contribution

$$a_\mu^{(4)\,\rm EW}([f]) \simeq \frac{\sqrt{2}G_\mu m_\mu^2}{16\pi^2}\,\frac{\alpha}{\pi}\,2T_{3f}N_{\rm cf}Q_{\rm f}^2\ \left[3\ln\frac{M_{\rm Z}^2}{m_{\rm f'}^2} + C_{\rm f}\right] \tag{27}$$

where $T_{3\rm f}$ is the third component of the weak isospin, $Q_{\rm f}$ the charge and $N_{\rm cf}$ the color factor, 1 for leptons, 3 for quarks. The mass $m_{\rm f'}$ is m_μ if $m_{\rm f} < m_\mu$

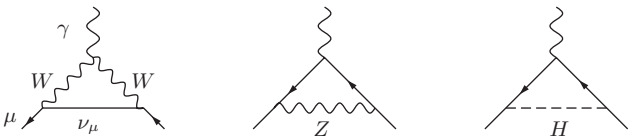

Fig. 2. The leading weak contributions to a_ℓ; diagrams in the physical unitary gauge

and $m_{\rm f}$ if $m_{\rm f} > m_\mu$, and $C_{\rm e} = 5/2,\ C_\mu = 11/6 - 8/9\,\pi^2,\ C_\tau = -6$ [41]. However, in the SM the consideration of individual fermions makes no sense and a separation of quarks and leptons in not possible. Mathematical consistency of the SM requires complete VVA anomaly cancellation between lepton and quark and actually $\sum_f N_{\rm cf} Q_{\rm f}^2 T_{3\rm f} = 0$ holds for each of the three known lepton–quark families separately. Indeed, the $\sim \ln M_{\rm Z}$ terms cancel if quarks are treated as free fermions [42]. However, strong interaction effects must be included as well.

In fact, low-energy QCD is characterized in the *chiral limit* of massless light quarks u,d,s, by *spontaneous chiral symmetry breaking* (SχSB) of the chiral group $SU(3)_V \otimes SU(3)_A$, which in particular implies the existence of the pseudo-scalar octet of pions and kaons as Goldstone bosons. The light quark condensates are essential features in this situation and lead to non-perturbative effects completely absent in a perturbative approach. Thus low-energy QCD effects are intrinsically non-perturbative and controlled by chiral perturbation theory (CHPT), the systematic QCD low-energy expansion, which accounts for the SχSB and the chiral symmetry breaking by quark masses in a systematic manner. The low-energy effective theory describing the hadronic contributions related to the light quarks u,d,s requires the calculation of the diagrams of the type shown in Fig. 3. The leading effect for the first plus second family takes the form [43]

$$a_\mu^{(4)\,\rm EW}\left(\begin{bmatrix} e,u,d \\ \mu,c,s \end{bmatrix}\right)_{\rm CHPT} = \frac{\sqrt{2}G_\mu\, m_\mu^2}{16\pi^2}\,\frac{\alpha}{\pi}\left[-\frac{14}{3}\ln\frac{M_\Lambda^2}{m_\mu^2} + 4\ln\frac{M_\Lambda^2}{m_c^2} - \frac{35}{3} + \frac{8}{9}\pi^2\right]$$
$$\simeq -\frac{\sqrt{2}G_\mu\, m_\mu^2}{16\pi^2}\,\frac{\alpha}{\pi}\times 26.2(5) \simeq -7.09(13)\times 10^{-11}. \quad (28)$$

The error comes from varying the cut-off M_Λ between 1 and 2 GeV. Below 1 GeV CHPT can be trusted above 2 GeV we can trust pQCD. Fortunately the result is not very sensitive to the choice of the cut-off. For more sophisticated analyses we refer to [42, 43, 44] which was corrected and refined in [45, 46]. Thereby, a new kind of non-renormalization theorems played a key role [47, 48, 49]. Including subleading effects yields -5.0×10^{-11} for the first two families. The third family of fermions including the heavy top quark can be treated in perturbation theory and was worked out to

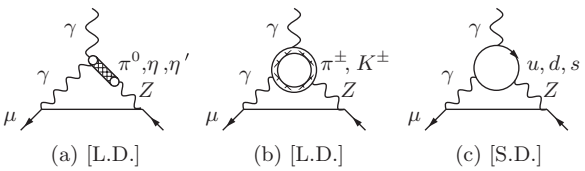

Fig. 3. The two leading CHPT diagrams (L.D.) and the QPM diagram (S.D.). The charged pion loop is sub-leading and is actually discarded. Diagrams with permuted $\gamma \leftrightarrow$ Z on the μ-line have to be included

be -8.2×10^{-11} in [50]. Subleading fermion-loops contribute -5.3×10^{-11}. There are many more diagrams contributing, in particular the calculation of the bosonic contributions (1678 diagrams) is a formidable task and has been performed by Czarnecki, Krause and Marciano (1996) as an expansion in $(m_\mu/M_V)^2$ and $(M_V/m_H)^2$ [51]. Later complete calculations, valid also for lighter Higgs masses, were performed [52, 53], which confirmed the previous result -22.3×10^{-11}.

The complete weak contribution may be summarized by [46]

$$\begin{aligned} a_\mu^{\rm EW} &= \frac{\sqrt{2}G_\mu\, m_\mu^2}{16\pi^2}\left\{\frac{5}{3}+\frac{1}{3}\,(1-4\sin^2\Theta_W)^2-\frac{\alpha}{\pi}[155.5(4)(2)]\right\} \\ &= (154\pm 1[\text{had}]\pm 2[m_H, m_t, \text{3-loop}])\times 10^{-11} \end{aligned} \tag{29}$$

with errors from triangle quark-loops and from variation of the Higgs mass in the range $m_H = 150^{+100}_{-40}$ GeV. The 3-loop effect has been estimated to be negligible [45, 46].

3.4 Hadronic Contributions

So far when we were talking about fermion-loops we only considered the lepton loops. Besides the leptons the strongly interacting quarks also have to be taken into account. The problem is that strong interactions at low energy are non-perturbative and straightforward first principle calculations become very difficult and often impossible.

Fortunately the leading hadronic effects are vacuum polarization type corrections, which can be safely evaluated by exploiting causality (analyticity) and unitarity (optical theorem) together with experimental low-energy data. The imaginary part of the photon self-energy function $\Pi_\gamma(s)$ is determined via the optical theorem by the total cross-section of hadron production in electron–positron annihilation:

$$\sigma(s)_{e^+e^-\to\gamma^*\to\text{hadrons}} = \frac{4\pi^2\alpha}{s}\,\frac{1}{\pi}\,\text{Im}\,\Pi_\gamma(s)\ . \tag{30}$$

The leading hadronic contribution is represented by Fig. 4, which has a representation as a dispersion integral

$$a_\mu = \frac{\alpha}{\pi}\int_0^\infty \frac{ds}{s}\,\frac{1}{\pi}\,\text{Im}\,\Pi_\gamma(s)\,K(s)\ ,\quad K(s)\equiv\int_0^1 dx\frac{x^2(1-x)}{x^2+\frac{s}{m_\mu^2}(1-x)}\ . \tag{31}$$

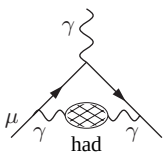

Fig. 4. The leading order (LO) hadronic vacuum polarization diagram

As a result the leading non-perturbative hadronic contributions $a_\mu^{\rm had}$ can be obtained in terms of $R_\gamma(s) \equiv \sigma^{(0)}(e^+e^- \to \gamma^* \to \text{hadrons})/\frac{4\pi\alpha^2}{3s}$ data via the dispersion integral:

$$a_\mu^{\rm had} = \left(\frac{\alpha m_\mu}{3\pi}\right)^2 \left(\int\limits_{4m_\pi^2}^{E^2_{\rm cut}} {\rm d}s \, \frac{R_\gamma^{\rm data}(s)\, \hat{K}(s)}{s^2} + \int\limits_{E^2_{\rm cut}}^{\infty} {\rm d}s \, \frac{R_\gamma^{\rm pQCD}(s)\, \hat{K}(s)}{s^2} \right). \quad (32)$$

The rescaled kernel function $\hat{K}(s) = 3s/m_\mu^2\, K(s)$ is a smooth bounded function, increasing from 0.63... at $s = 4m_\pi^2$ to 1 as $s \to \infty$. The $1/s^2$ enhancement at low energy implies that the $\rho \to \pi^+\pi^-$ resonance is dominating the dispersion integral ($\sim 75\%$). Data can be used up to energies where $\gamma - Z$ mixing comes into play at about 40 GeV. However, by virtue of asymptotic freedom, perturbative quantum chromodynamics (pQCD) becomes more reliable the higher the energy and in fact may be used safely in regions away from the flavor thresholds where the non-perturbative resonances show up: ρ, ω, ϕ, the J/ψ series and the Υ series. We thus use perturbative QCD [54, 55] from 5.2 to 9.6 GeV and for the high-energy tail above 13 GeV, as recommended in [54, 55].

Hadronic cross-section measurements $e^+e^- \to$ hadrons at electron–positron storage rings started in the early 1960s and continued up to date. Since our analysis [56] in 1995 data from MD1 [57], BES-II [58] and from CMD-2 [59] have led to a substantial reduction in the hadronic uncertainties on $a_\mu^{\rm had}$. More recently, KLOE [60], SND [61] and CMD-2 [62] published new measurements in the region below 1.4 GeV. My up-to-date evaluation of the leading order hadronic VP yields [63]

$$a_\mu^{\rm had(1)} = (692.1 \pm 5.6) \times 10^{-10} \, . \quad (33)$$

Some other recent evaluations are collected in Table 1. Differences in errors come about mainly by utilizing more "theory-driven" concepts : use of selected

Table 1. Some recent evaluations of $a_\mu^{\rm had(1)}$

$a_\mu^{\rm had(1)} \times 10^{10}$	data	Reference
696.3[7.2]	e^+e^-	[64]
711.0[5.8]	$e^+e^- + \tau$	[64]
694.8[8.6]	e^+e^-	[65]
684.6[6.4]	e^+e^- TH	[66]
699.6[8.9]	e^+e^-	[67]
692.4[6.4]	e^+e^-	[68]
693.5[5.9]	e^+e^-	[69]
701.8[5.8]	$e^+e^- + \tau$	[69]
690.9[4.4]	e^+e^{-**}	[70]
692.1[5.6]	e^+e^{-**}	[63]

data sets only, extended use of perturbative QCD in place of data [assuming local quark-hadron duality], sum rule methods, low-energy effective methods. Only the last two (**) results include the most recent data from SND, CMD-2 and BaBar.

In principle, the $I = 1$ iso-vector part of $e^+e^- \to$ hadrons can be obtained in an alternative way by using the precise vector spectral functions from hadronic τ-decays $\tau \to \nu_\tau +$ hadrons which are related by an isospin rotation [71]. After isospin violating corrections, due to photon radiation and the mass splitting $m_d - m_u \neq 0$, have been applied, there remains an unexpectedly large discrepancy between the e^+e^-- and the τ-based determinations of a_μ [64], as may be seen in Table 1. Possible explanations are so far unaccounted isospin breaking [65] or experimental problems with the data. Since the e^+e^-- data are more directly related to what is required in the dispersion integral, one usually advocates to use the e^+e^- data only.

At order $O(\alpha^3)$ diagrams of the type shown in Fig. 5 have to be calculated, where the first diagram stands for a class of higher order hadronic contributions obtained if one replaces one internal photon line by a dressed one in any of the 6-two loop diagrams which do not exhibit a fermion loop. The relevant kernels for the corresponding dispersion integrals have been calculated analytically in [72] and appropriate series expansions were given in [73] (for earlier estimates see [74, 75]). Based on my recent compilation of the e^+e^- data [63] I obtain

$$a_\mu^{\mathrm{had}(2)} = (-100.3 \pm 2.2) \times 10^{-11} \,, \tag{34}$$

in accord with previous evaluations [75, 73, 71, 68].

We encounter much more serious problems with non-perturbative hadronic effect with the hadronic light-by-light (LbL) contribution at $O(\alpha^3)$ depicted in Fig. 6. Experimentally, we know that $\gamma\gamma \to$ hadrons $\to \gamma\gamma$ is dominated by the hadrons π^0, η, η', ..., i.e., single pseudo-scalar meson spikes, and that $\pi^0 \to \gamma\gamma$, etc., is governed by the parity odd Wess-Zumino-Witten (WZW) effective Lagrangian

$$\mathcal{L}^{(4)} = -\frac{\alpha N_c}{12\,\pi f_0} \varepsilon_{\mu\nu\rho\sigma} F^{\mu\nu} A^\rho \partial^\sigma \pi^0 + \cdots \tag{35}$$

which reproduces the Adler-Bell-Jackiw triangle anomaly and which helps in estimating the leading hadronic LbL contribution. f_0 denotes the pion decay constant f_π in the chiral limit of massless light quarks. Again, in a low-energy

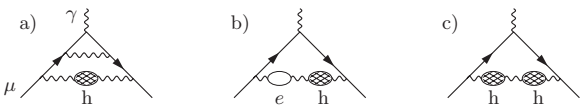

Fig. 5. Higher order (HO) vacuum polarization contributions

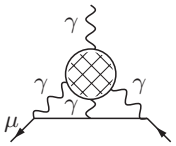

Fig. 6. Hadronic light-by-light scattering in $g-2$

effective description, the quasi Goldstone bosons, the pions and kaons play an important role, and the relevant diagrams are displayed in Fig. 7.

However, as we know from the hadronic VP discussion, the ρ meson is expected to play an important role in the game. It looks natural to apply a vector-meson dominance (VMD) like model. Electromagnetic interactions of pions treated as point-particles would be described by scalar QED in a first step. However, due to hadronic interactions the photon mixes with hadronic vector-mesons like the ρ^0, which is properly accommodated by the Resonance Lagrangian Approach (RLA) [76] or versions of it, an extended version of CHPT which incorporates vector-mesons in accordance with the basic symmetries.

Based on such effective field theory (EFT) models, two major efforts in evaluating the full a_μ^{LbL} contribution were made by Hayakawa, Kinoshita and Sanda (HKS 1995) [77], Bijnens, Pallante and Prades (BPP 1995) [78] and Hayakawa and Kinoshita (HK 1998) [79] (see also Kinoshita, Nizic and Okamoto (KNO 1985) [75]). Although the details of the calculations are quite different, which results in a different splitting of various contributions, the results are in good agreement and essentially given by the π^0-pole contribution, which was taken with the wrong sign, however. In order to eliminate the cut-off dependence in separating L.D. and S.D. physics, more recently it became favorable to use quark–hadron duality, as it holds in the large N_c limit of QCD, for modeling of the hadronic amplitudes [80]. The infinite series of narrow vector states known to show up in the large N_c limit is then approximated by a suitable lowest meson dominance (LMD+V) Ansatz [81], assumed to be saturated by known low-lying physical states of appropriate quantum numbers. This approach was adopted in a reanalysis by Knecht and Nyffeler (KN 2001) [82, 83, 84] in 2001, in which they discovered a sign mistake

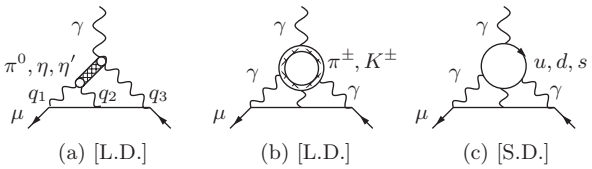

Fig. 7. Leading hadronic light-by-light scattering diagrams: the two leading CHPT diagrams (L.D.) and the QPM diagram (S.D.). The charged pion loop is subleading only, actually. Diagrams with permuted γs on the μ-line have to be included. γ-hadron/quark vertices at $q^2 \neq 0$ are dressed (VMD)

in the dominant π^0, η, η' exchange contribution, which changed the central value by $+167 \times 10^{-11}$, a 2.8 σ shift, and which reduces a larger discrepancy between theory and experiment. More recently, Melnikov and Vainshtein (MV 2004) [85] found additional problems in previous calculations, this time in the short distance constraints (QCD/OPE) used in matching the high-energy behavior of the effective models used for the π^0, η, η' exchange contribution.

The most important pion-pole term, Fig. 7(a), exhibits the non-perturbative aspects in a product of two essentially unknown $\pi^0\gamma\gamma$ form factors (FF) like $\mathcal{F}_{\pi^*\gamma^*\gamma^*}(q_2^2, q_1^2, q_3^2) \cdot \mathcal{F}_{\pi^*\gamma^*\gamma^*}(q_2^2, q_2^2, 0)$ where the photon momenta q_1 and q_2 are the loop momenta to be integrated over.

A new quality of the problem encountered here is the fact that the integrand depends on three invariants q_1^2, q_2^2, q_3^2 with $q_3 = -(q_1 + q_2)$, while hadronic VP correlators or the VVA triangle with an external zero momentum vertex only depends on a single invariant q^2. In the latter case the invariant amplitudes (form factors) may be separated into a low-energy part $q^2 \leq \Lambda^2$ (soft) where the low-energy effective description applies and a high-energy part $q^2 > \Lambda^2$ (hard) where pQCD works. In multi-scale problems, however, there are mixed soft–hard regions where no answer is available in general, unless we have data to constrain the amplitudes in such regions. In our case, only the soft region $q_1^2, q_2^2, q_3^2 \leq \Lambda^2$ and the hard region $q_1^2, q_2^2, q_3^2 > \Lambda^2$ are under control of either the low-energy EFT or pQCD, respectively. In the mixed soft–hard domains operator product expansions and/or soft versus hard factorization "theorems" may apply. Actually, one more approximation is usually made: the *pion-pole approximation*, i.e., the pion-momentum square (first argument of the $\mathcal{F}$) is set equal to m_π^2, as the main contribution is expected to come from the pole. Knecht and Nyffeler modeled $\mathcal{F}_{\pi\gamma^*\gamma^*}(m_\pi^2, q_1^2, q_2^2)$ in the spirit of the large N_c expansion as a "LMD+V" form factor:

$$\mathcal{F}_{\pi\gamma^*\gamma^*}(m_\pi^2, q_1^2, q_2^2) = \frac{f_\pi}{3} \frac{q_1^2 q_2^2 (q_1^2 + q_2^2) + h_1 (q_1^2 + q_2^2)^2 + h_2 q_1^2 q_2^2 + h_5 (q_1^2 + q_2^2) + h_7}{(q_1^2 - M_1^2)(q_1^2 - M_2^2)(q_2^2 - M_1^2)(q_2^2 - M_2^2)}, \tag{36}$$

with $h_7 = -(N_c M_1^4 M_2^4 / 4\pi^2 f_\pi^2)$, $f_\pi \simeq 92.4$ MeV. An important constraint comes from the pion-pole form factor $\mathcal{F}_{\pi\gamma^*\gamma}(m_\pi^2, -Q^2, 0)$, which has been measured by CELLO [86] and CLEO [87]. Experiments are in fair agreement with the Brodsky–Lepage [88] form

$$\mathcal{F}_{\pi\gamma^*\gamma}(m_\pi^2, -Q^2, 0) \simeq -\frac{N_c}{12\pi^2 f_\pi} \frac{1}{1 + (Q^2/8\pi^2 f_\pi^2)} \tag{37}$$

which interpolates between a $1/Q^2$ asymptotic behavior and the constraint from π^0 decay at $Q^2 = 0$. This behavior requires $h_1 = 0$. Identifying the resonances with $M_1 = M_\rho = 769$ MeV, $M_2 = M_{\rho'} = 1465$ MeV, the phenomenological constraint fixes $h_5 = 6.93$ GeV^4. h_2 will be fixed by later. As the previous analyses, Knecht and Nyffeler apply the above VMD-type form factor on both ends of the pion line. In fact at the vertex attached to the external zero momentum photon, this type of pion-pole form factor cannot

apply for kinematical reasons: when $q^\mu_{\rm ext} = 0$ not $\mathcal{F}_{\pi\gamma^*\gamma}(m_\pi^2, -Q^2, 0)$ but $\mathcal{F}_{\pi^*\gamma^*\gamma}(q_2^2, q_2^2, 0)$ is the relevant object to be used, where q_2 is to be integrated over. However, for large q_2^2 the pion must be far off-shell, in which case the pion exchange effective representation becomes obsolete. Melnikov and Vainshtein reanalyzed the problem by performing an operator product expansion (OPE) for $q_1^2 \simeq q_2^2 \gg (q_1+q_2)^2 \sim m_\pi^2$. In the chiral limit this analysis reveals that the external vertex is determined by the exactly known ABJ anomaly $\mathcal{F}_{\pi\gamma\gamma}(m_\pi^2, 0, 0) = -1/(4\pi^2 f_\pi)$. This means that in the chiral limit there is no VMD-like damping at high energies at the external vertex. However, the absence of a damping in the chiral limit does not prove that there is no damping in the real world with non-vanishing quark masses. In fact, the quark triangle-loop in this case provides a representation of the $\pi^{0*}\gamma^*\gamma^*$ amplitude given by

$$F^{\rm CQM}_{\pi^{0*}\gamma^*\gamma^*}(q^2, p_1^2, p_2^2) \equiv (-4\pi^2 f_\pi)\, \mathcal{F}_{\pi^*\gamma^*\gamma^*}(q^2, p_1^2, p_2^2) = 2m_{\rm q}^2\, C_0(m_{\rm q}; q^2, p_1^2, p_2^2)\ ,$$

where C_0 is a well-known scalar 3-point function and $m_{\rm q}$ is a quark mass (q=u,d,s). For $p_1^2 = p_2^2 = q^2 = 0$ we obtain $F^{\rm CQM}_{\pi^{0*}\gamma^*\gamma^*}(0,0,0) = 1$, which is the proper ABJ anomaly. For large p_1^2 at $p_2^2 \sim 0,\ q^2 \sim 0$ or $p_1^2 \sim p_2^2$ at $q^2 \sim 0$ the asymptotic behavior is given by

$$F^{\rm CQM}_{\pi^0\gamma^*\gamma}(0, p_1^2, 0) \sim r\ \ln^2 r\ ,\ \ F^{\rm CQM}_{\pi^0\gamma^*\gamma^*}(0, p_1^2, p_1^2) \sim 2\, r\ \ln r, \tag{38}$$

where $r = \frac{m_{\rm q}^2}{-p_1^2}$. As C_0 is permutation symmetric the same power behavior $\sim 1/p_i^2$ modulo logarithms holds in all channels. Thus at high energies the anomaly gets screened by chiral symmetry breaking effects.

We therefore advocate to use consistently dressed form factors as inferred by the resonance Lagrangian approach. However, other effects which were first considered in [85] must be taken into account:

1) The constraint on the twist four $(1/q^4)$-term in the OPE requires $h_2 = -10$ GeV^2 in the Knecht–Nyffeler form factor (36): $\delta a_\mu \simeq +5 \pm 0$.
2) The contributions from the f_1 and f_1' isoscalar axial-vector mesons: $\delta a_\mu \simeq +10 \pm 4$ (using dressed photons).
3) For the remaining effects: scalars (f_0) + dressed $\pi^\pm, K^\pm$ loops + dressed quark loops: $\delta a_\mu \simeq -5 \pm 13$.

Note that the remaining terms have been evaluated in [77, 78] only. The splitting into the different terms is model dependent and only the sum should be considered: the results read -5 ± 13 (BPP) and 5.2 ± 13.7 (HKS) and hence the contribution remains unclear[4].

Results are overviewed in Table 2. The last column gives my estimates based on [77, 78, 82, 85]. The "no FF" column shows results for undressed photons (no form factor). The constant WZW form factor yields a divergent

[4] We adopt the value estimated in [78], because the sign of the scalar contribution, which dominates in the sum, has to be negative in any case (see [84]).

Table 2. LbL: Summary of most recent results for $a_\mu \times 10^{11}$

	no FF	BPP	HKS	KN	MV	FJ
π^0, η, η'	$+\infty$	85 ± 13	82.7 ± 6.4	83 ± 12	114 ± 10	88 ± 12
axial-vector		2.5 ± 1.0	1.7 ± 0.0		22 ± 5	10 ± 4
scalar		-6.8 ± 2.0	–	–	–	-7 ± 2
π, K loops	-49.8	-19 ± 13	-4.5 ± 8.1		0 ± 10	-19 ± 13
quark loops	62(3)	21 ± 3	9.7 ± 11.1	–	–	21 ± 3
total		83 ± 32	89.6 ± 15.4	80 ± 40	136 ± 25	93 ± 34

result; applying a cut-off Λ one obtains [83] $(\alpha/\pi)^3 \mathcal{C} \ln^2 \Lambda$, with an universal coefficient $\mathcal{C} = N_c^2 m_\mu^2/(48\pi^2 f_\pi^2)$; in the VMD dressed cases M_V represents the cut-off $\Lambda \to M_V$ if $M_V \to \infty$.

4 Theory Confronting the Experiment

The following Table 3 collects the typical contributions to a_μ evaluated in terms of α determined via a_e (13). The world average experimental muon magnetic anomaly, dominated by the very precise BNL result, now is [8]

$$a_\mu^{\rm exp} = 1.16592080(60) \times 10^{-3} \tag{39}$$

(relative uncertainty 5.3×10^{-7}), which confronts with the SM prediction

$$a_\mu^{\rm the} = 1.16591793(68) \times 10^{-3}\,. \tag{40}$$

Figure 8 illustrates the improvement achieved by the BNL experiment. The theoretical predictions mainly differ by the L.O. hadronic effects, which also dominate the theoretical error. A deviation between theory and experiment

Table 3. The various types of contributions to a_μ in units 10^{-6}, ordered according to their size (L.O. lowest order, H.O. higher order, LbL. light–by–light)

L.O. universal	1161.409 73	(0)
e-loops	6.194 57	(0)
H.O. universal	−1.757 55	(0)
L.O. hadronic	0.069 20	(56)
L.O. weak	0.001 95	(0)
H.O. hadronic	−0.001 00	(2)
LbL. hadronic	0.001 00	(39)
τ-loops	0.000 43	(0)
H.O. weak	−0.000 41	(2)
e+τ-loops	0.000 01	(0)
theory	1165.917 93	(68)
experiment	1165.920 80	(60)

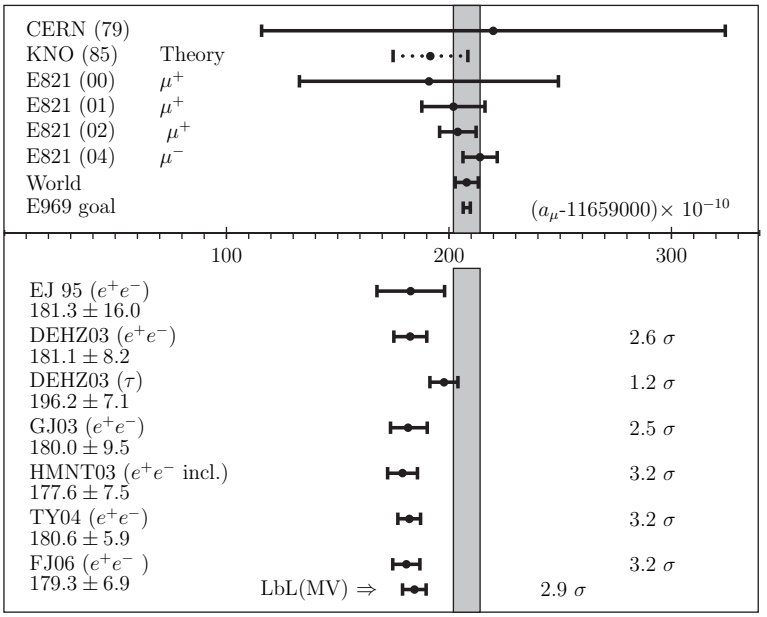

Fig. 8. Comparison between theory and experiment. Results differ by different L.O. hadronic vacuum polarizations, except for the last point which includes the Melnikov-Vainshtein estimate of the LbL contribution. EJ95 vs. FJ06 illustrates the improvement of the e^+e^--data between 1995 and now (see also Table 1)

of about 3 σ was persisting since the first precise BNL results came out, in spite of progress in theory and experiment since.

At present the deviation between theory and experiment is

$$\delta a_\mu = a_\mu^{\rm exp} - a_\mu^{\rm the} = 287 \pm 91 \times 10^{-11}, \tag{41}$$

which is a 3.2 σ effect. We note that the theory error is somewhat larger than the experimental one. It is fully dominated by the uncertainty of the hadronic low-energy cross-section data, which determine the hadronic vacuum polarization and, partially, form the uncertainty of the hadronic light-by-light scattering contribution.

As we notice, the enhanced sensitivity to "heavy" physics is somehow good news and bad news at the same time: the sensitivity to "New Physics" we are always hunting for at the end is enhanced due to

$$a_\ell^{\rm NP} \sim \left(\frac{m_\ell}{M_{\rm NP}}\right)^2$$

by the mentioned mass ratio square, but at the same time also scale-dependent SM effects are dramatically enhanced, and the hadronic ones are not easy to estimate with the desired precision.

5 Prospects

The BNL muon $g-2$ experiment has determined a_μ (39), reaching the impressive precision of 0.54 ppm, a 14-fold improvement over the CERN experiment from 1976. Herewith, a new quality has been achieved in testing the SM and in limiting physics beyond it. The main achievements and problems are

- a first confirmation of the fairly small weak contribution at the 2–3 σ level,
- a substantial improvement in testing CPT $a_{\mu^+} = a_{\mu^-}$ for muons,
- the hadronic vacuum polarization contribution, obtained via experimental e^+e^- annihilation data, limits the theoretical precision at the 1 σ level,
- now and for the future the hadronic light-by-light scattering contribution, which amounts to about 2σ, is not far from being as important as the weak contribution; present calculations are model-dependent and may become the limiting factor for future progress.

At present a 3.2σ deviation between theory and experiment is observed[5] and the "missing piece" (41) could hint to new physics, but at the same time rules out big effects predicted by many possible extensions of the SM.

Usually, new physics (NP) contributions due to not yet seen heavy states via virtual corrections are expected to produce contributions proportional to $m_\mu^2/M_{\rm NP}^2$ and thus are expected to be suppressed by $M_{\rm W}^2/M_{\rm NP}^2$ relative to the weak contribution.

The most promising theoretical scenarios are super symmetric (SUSY) extensions of the SM, in particular the minimal MSSM. Typical super-symmetric contributions to a_μ stem from smuon–neutralino and sneutrino-chargino loops Fig. 9. Some contributions are enhanced by the parameter $\tan\beta$ which may be large (in some cases of order $m_t/m_b \approx 40$). One obtains [89] (for the extension to 2-loops see [90])

$$a_\mu^{\rm SUSY} \simeq {\rm sign}(\mu)\frac{\alpha(M_{\rm Z})}{8\pi\sin^2\Theta_W}\frac{m_\mu^2}{\widetilde{m}^2}\tan\beta\left(1-\frac{4\alpha}{\pi}\ln\frac{\widetilde{m}}{m_\mu}\right), \tag{42}$$

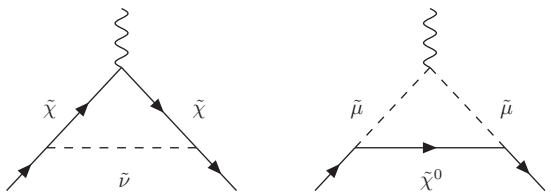

Fig. 9. Physics beyond the SM: leading SUSY contributions to $g-2$ in supersymmetric extension of the SM

[5] It is the largest established deviation between theory and experiment in electroweak precision physics at present.

$\widetilde{m} = m_{\rm SUSY}$ a typical SUSY loop mass and μ is the Higgsino mass term. In view of (41) negative μ models give the opposite sign contribution to a_μ and are strongly disfavored. For $\tan\beta$ in the range 3–40 one obtains

$$\widetilde{m} \simeq 110\text{–}430 \text{ GeV}, \tag{43}$$

precisely the range where SUSY particles are often expected. For a variety of non-SUSY extensions of the SM typically $\left|a_\mu(\text{NP})\right| \simeq \mathcal{C}\, m_\mu^2/M^2$ where $\mathcal{C} = O(1)$ [or $O(\alpha/\pi)$ if radiatively induced]. The current constraint suggests $M \simeq 1.5\text{–}2.5\text{TeV}[M \simeq 80\text{–}120\text{GeV}]$. Note that $\mathcal{C} = O(1)$ could be in conflict with the requirement that no tree level contribution is allowed. For a more elaborate discussion and further references I refer to [91].

Plans for a new $g-2$ experiment exist [92]. In fact, the impressive 0.5 ppm precision measurement by the E821collaboration at Brookhaven was still limited by statistical errors rather than by systematic ones. Therefore an upgrade of the experiment at Brookhaven or J-PARC (Japan) is supposed to be able to reach a precision of 0.2 ppm (Brookhaven) or 0.1 ppm (J-PARC).

For the theory this poses a new challenge. It is clear that on the theory side, a reduction of the leading hadronic uncertainty is required, which actually represents a big experimental challenge: one has to attempt cross-section measurements at the 1% level up to $J/\psi[\Upsilon]$ energies (5[10] GeV). Such measurements would be crucial for the muon $g-2$ as well as for a more precise determination of the running fine structure constant $\alpha_{\rm QED}(E)$. In particular, e^+e^- low-energy cross-section measurements in the region between 1 and 2.5 GeV [93, 94] are able to substantially improve the accuracy of $a_\mu^{\rm had(1)}$ and $\alpha_{\rm QED}(M_Z)$ [63].

New ideas are required to get less model-dependent estimations of the hadronic LbL contribution.

In any case the muon $g-2$ story is a beautiful example which illustrates the experience that the closer we look the more there is to see, but also the more difficult it gets to predict and interpret what we see. Even facing problems to pin down precisely the hadronic effects, the achievements in the muon $g-2$ is a big triumph of science. Here all kinds of physics meet in one number which is the result of a truly ingenious experiment. Only getting all details in all aspects correct makes this number a key quantity for testing our present theoretical framework in full depth. It is the result of tremendous efforts in theory and experiment and on the theory side has triggered the development of new methods and tools such as computer algebra as well as high-precision numerical methods which are indispensable to handle the complexity of hundreds to thousands of high-dimensional integrals over singular integrands suffering from huge cancellations of huge numbers of terms. Astonishing that all this really works!

Acknowledgments

It is a pleasure to thank the organizers of PSAS 2006 and in particular to Savely Karshenboim for the kind invitation to this stimulating meeting. Thanks also to Oleg Tarsov and Rainer Sommer for helpful discussions and for carefully reading the manuscript. This work was supported in part by EC-Contracts HPRN-CT-2002-00311 (EURIDICE) and RII3-CT-2004-506078 (TARI).

References

1. P. A. M. Dirac: Proc. Roy. Soc. A **117**, 610 (1928); A **118**, 351 (1928).
2. P. Kusch, H. M. Foley: Phys. Rev. **73**, 421 (1948); Phys. Rev. **74**, 250 (1948).
3. J. S. Schwinger: Phys. Rev. **73**, 416 (1948).
4. G. Charpak et al.: Phys. Lett. **1**, 16 (1962).
5. J. Bailey et al.: Nuovo Cimento A **9**, 369 (1972).
6. J. Aldins et al.: Phys. Rev. Lett. **23**, 441 (1969); Phys. Rev. D **1**, 2378 (1970).
7. J. Bailey et al.: Nucl. Phys. B **150**, 1 (1979).
8. R. M. Carey et al.: Phys. Rev. Lett. **82**, 1632 (1999); H. N. Brown et al.: Phys. Rev. D **62**, 091101 (2000); Phys. Rev. Lett. **86**, 2227 (2001); G. W. Bennett et al.: Phys. Rev. Lett. **89**, 101804 (2002)[Erratum: Phys. Rev. Lett. **89**, 129903 (2002)]; Phys. Rev. Lett. **92**, 161802 (2004).
9. B. Odom et al.: Phys. Rev. Lett. **97**, 030801 (2006).
10. G. Gabrielse et al.: Phys. Rev. Lett. **97**, 030802 (2006) [Erratum-ibid. **99**, 039902 (2007)].
11. S. Eidelman et al.: [Particle Data Group], Phys. Lett. B **592**, 1 (2004).
12. P. J. Mohr, B. N. Taylor, Rev. Mod. Phys. **72**, 351 (2000); **77**, 1 (2005).
13. A. Petermann: Helv. Phys. Acta **30**, 407 (1957); Nucl. Phys. **5**, 677 (1958).
14. C. M. Sommerfield: Phys. Rev. **107**, 328 (1957); Ann. Phys. (N.Y.) **5**, 26 (1958).
15. S. Laporta, E. Remiddi: Phys. Lett. B **379**, 283 (1996).
16. T. Kinoshita: Phys. Rev. Lett., **75**, 4728 (1995).
17. T. Kinoshita, W. B. Lindquist: Phys. Rev. D **27**, 867 (1983); **27**, 877 (1983); **27**, 886 (1983); **39**, 2407 (1989); **42**, 636 (1990).
18. V. W. Hughes, T. Kinoshita: Rev. Mod. Phys. **71**, S133 (1999).
19. T. Kinoshita, M. Nio: Phys. Rev. D **73**, 013003 (2006).
20. T. Aoyama, M. Hayakawa, T. Kinoshita, M. Nio, Phys. Rev. Lett. **99**, 110406 (2007).
21. P. J. Mohr, B. N. Taylor: Rev. Mod. Phys. **77**, 1 (2005).
22. H. Suura, E. Wichmann: Phys. Rev., **105**, 1930 (1957); A. Petermann: Phys. Rev. **105**, 1931 (1957).
23. H. H. Elend: Phys. Lett. **20**, 682 (1966) [Erratum: Phys. Lett. **21**, 720 (1966)].
24. B. E. Lautrup, E. De Rafael: Nuovo Cim. A **64**, 322 (1969).
25. B. Lautrup: Phys. Lett. B **69**, 109 (1977).
26. G. Li, R. Mendel, M. A. Samuel: Phys. Rev. D **47**, 1723 (1993).
27. T. Kinoshita: Nuovo Cim. B **51**, 140 (1967).
28. B. E. Lautrup, E. De Rafael: Phys. Rev. **174**, 1835 (1968); B. E. Lautrup, M. A. Samuel: Phys. Lett. B **72**, 114 (1977).

29. M. A. Samuel, G. Li: Phys. Rev. D **44**, 3935 (1991) [Errata: Phys. Rev. D **46**, 4782 (1992); D **48**, 1879 (1993)].
30. S. Laporta: Nuovo Cim. A **106**, 675 (1993).
31. S. Laporta, E. Remiddi: Phys. Lett. B **301**, 440 (1993).
32. J. H. Kühn et al.: Phys. Rev. D **68**, 033018 (2003).
33. A. Czarnecki, M. Skrzypek: Phys. Lett. B **449**, 354 (1999).
34. S. Friot, D. Greynat, E. De Rafael: Phys. Lett. B **628**, 73 (2005).
35. M. Passera: J. Phys. G **31**, R75 (2005); Phys. Rev. D **75**, 013002 (2007).
36. M. Caffo, S. Turrini, E. Remiddi: Phys. Rev. D **30**, 483 (1984); E. Remiddi, S. P. Sorella: Lett. Nuovo Cim. **44**, 231 (1985); D. J. Broadhurst, A. L. Kataev, O. V. Tarasov: Phys. Lett. B **298**, 445 (1993); S. Laporta: Phys. Lett. B **312**, 495 (1993); P. A. Baikov, D. J. Broadhurst: hep-ph/9504398.
37. T. Kinoshita, M. Nio: Phys. Rev. Lett. **90**, 021803 (2003); Phys. Rev. D **70**, 113001 (2004).
38. S. G. Karshenboim: Phys. Atom. Nucl. **56**, 857 (1993).
39. T. Kinoshita, M. Nio: Phys. Rev. D **73**, 053007 (2006).
40. A. L. Kataev: Nucl. Phys. Proc. Suppl. **155**, 369 (2006); hep-ph/0602098; Phys. Rev. D **74**, 073011 (2006).
41. E. A. Kuraev, T. V. Kukhto, A. Schiller: Sov. J. Nucl. Phys. **51**, 1031 (1990); T. V. Kukhto et al.: Nucl. Phys. **B 371**, 567 (1992).
42. A. Czarnecki, B. Krause, W. Marciano: Phys. Rev. D **52**, R2619 (1995).
43. S. Peris, M. Perrottet, E. de Rafael: Phys. Lett. B **355**, 523 (1995).
44. M. Knecht, S. Peris, M. Perrottet, E. de Rafael: JHEP **0211**, 003 (2002).
45. G. Degrassi, G. F. Giudice: Phys. Rev. **58**D, 053007 (1998).
46. A. Czarnecki, W. J. Marciano, A. Vainshtein: Phys. Rev. D **67**, 073006 (2003).
47. A. Vainshtein: Phys. Lett. B **569**, 187 (2003).
48. M. Knecht, S. Peris, M. Perrottet, E. de Rafael: JHEP **0403**, 035 (2004).
49. F. Jegerlehner, O. V. Tarasov: Phys. Lett. B **639**, 299 (2006).
50. E. D'Hoker: Phys. Rev. Lett. **69**, 1316 (1992).
51. A. Czarnecki, B. Krause, W. J. Marciano: Phys. Rev. Lett. **76**, 3267 (1996).
52. S. Heinemeyer, D. Stöckinger, G. Weiglein: Nucl. Phys. B **699**, 103 (2004).
53. T. Gribouk, A. Czarnecki: Phys. Rev. D **72**, 053016 (2005).
54. S. G. Gorishnii, A. L. Kataev, S. A. Larin: Phys. Lett. B **259**, 144 (1991); L. R. Surguladze, M. A. Samuel: Phys. Rev. Lett. **66**, 560 (1991) [Erratum: Phys. Rev. Lett. **66**, 2416 (1991)]; K. G. Chetyrkin: Phys. Lett. B **391**, 402 (1997).
55. K. G. Chetyrkin, J. H. Kühn: Phys. Lett. B **342**, 356 (1995); K. G. Chetyrkin, R. V. Harlander, J. H. Kühn: Nucl. Phys. B **586**, 56 (2000) [Erratum: Nucl. Phys. B **634**, 413 (2002)].
56. S. Eidelman, F. Jegerlehner: Z. Phys. C **67**, 585 (1995).
57. A. E. Blinov et al. [MD-1]: Z. Phys. C **70**, 31 (1996).
58. J. Z. Bai et al. [BES]: Phys. Rev. Lett. **84**, 594 (2000); Phys. Rev. Lett. **88**, 101802 (2002).
59. R. R. Akhmetshin et al. [CMD-2]: Phys. Lett. B **578**, 285 (2004); Phys. Lett. B **527**, 161 (2002).
60. A. Aloisio et al. [KLOE]: Phys. Lett. B **606**, 12 (2005).
61. M. N. Achasov et al. [SND]: J. Exp. Theor. Phys. **103**, 380 (2006).
62. V. M. Aulchenko et al. [CMD-2]: JETP Lett. **82**, 743 (2005); R. R. Akhmetshin et al.: JETP Lett. **84**, 413 (2006) [Pisma Zh. Eksp. Teor. Fiz. **84**, 491 (2006)]; Phys.

63. F. Jegerlehner: Nucl. Phys. Proc. Suppl. **162**, 22 (2006) [hep-ph/0608329].
64. M. Davier et al.: Eur. Phys. J. C **27**, 497 (2003); Eur. Phys. J. C **31**, 503 (2003).
65. F. Jegerlehner: J. Phys. G **29**, 101 (2003); S. Ghozzi, F. Jegerlehner: Phys. Lett. B **583**, 222 (2004).
66. S. Narison: Phys. Lett. B **568**, 231 (2003)
67. V. V. Ezhela, S. B. Lugovsky, O. V. Zenin: hep-ph/0312114.
68. K. Hagiwara et al.: Phys. Rev. D **69**, 093003 (2004).
69. J. F. de Troconiz, F. J. Yndurain: Phys. Rev. D **71**, 073008 (2005).
70. S. Eidelman et al.: ICHEP 2006 Moscow, (preliminary).
71. R. Alemany, M. Davier, A. Höcker: Eur. Phys. J. C **2**, 123 (1998).
72. R. Barbieri, E. Remiddi: Phys. Lett. B **49**, 468 (1974); Nucl. Phys. B **90**, 233 (1975).
73. B. Krause: Phys. Lett. B **390**, 392 (1997).
74. J. Calmet, S. Narison, M. Perrottet, E. de Rafael: Phys. Lett. B **61**, 283 (1976).
75. T. Kinoshita, B. Nizic, Y. Okamoto: Phys. Rev. D **31**, 2108 (1985).
76. G. Ecker, J. Gasser, A. Pich, E. de Rafael: Nucl. Phys. B **321**, 311 (1989); G. Ecker et al.: Phys. Lett. B **223**, 425 (1989).
77. M. Hayakawa, T. Kinoshita, A. I. Sanda: Phys. Rev. Lett. **75**, 790 (1995); Phys. Rev. D **54**, 3137 (1996).
78. J. Bijnens, E. Pallante, J. Prades: Phys. Rev. Lett. **75**, 1447 (1995) [Erratum: Phys. Rev. Lett. **75**, 3781 (1995)]; Nucl. Phys. B **474**, 379 (1996); [Erratum: Nucl. Phys. **626**, 410 (2002)].
79. M. Hayakawa, T. Kinoshita: Phys. Rev. D **57**, 465 (1998) [Erratum: Phys. Rev. D **66**, 019902 (2002)].
80. E. de Rafael: Phys. Lett. B **322**, 239 (1994).
81. S. Peris, M. Perrottet, E. de Rafael: JHEP **9805**, 011 (1998); M. Knecht, S. Peris, M. Perrottet, E. de Rafael: Phys. Rev. Lett. **83**, 5230 (1999); M. Knecht, A. Nyffeler: Eur. Phys. J. C **21**, 659 (2001).
82. M. Knecht, A. Nyffeler: Phys. Rev. D **65**, 073034 (2002).
83. M. Knecht, A. Nyffeler, M. Perrottet, E. De Rafael: Phys. Rev. Lett. **88**, 071802 (2002).
84. I. Blokland, A. Czarnecki, K. Melnikov: Phys. Rev. Lett. **88**, 071803 (2002).
85. K. Melnikov, A. Vainshtein: Phys. Rev. D **70**, 113006 (2004).
86. H. J. Behrend et al. [CELLO Collaboration]: Z. Phys. C **49**, 401 (1991).
87. J. Gronberg et al. [CLEO Collaboration]: Phys. Rev. D **57**, 33 (1998).
88. S. J. Brodsky, G. P. Lepage: Phys. Rev. D **24**, 1808 (1981).
89. T. Moroi,: Phys. Rev. D **53**, 6565 (1996) [Erratum: Phys. Rev. D **56**, 4424 (1997)].
90. S. Heinemeyer, D. Stöckinger, G. Weiglein: Nucl. Phys. B **690**, 62 (2004).
91. A. Czarnecki, W. J. Marciano: Phys. Rev. D **64**, 013014 (2001).
92. B. L. Roberts: Nucl. Phys. B (Proc. Suppl.) **131**, 157 (2004); R. M. Carey et al.: Proposal of the BNL Experiment E969, 2004; J-PARC Letter of Intent L17.
93. S. Eidelman, Physics at VEPP-2000, Nucl. Phys. Proc. Suppl. **162**, 323 (2006).
94. F. Ambrosino et al.: Prospects for e^+e^- physics at Frascati between the Φ and the ψ, Eur. Phys. J. C 50, 729 (2007); G. Venanzoni, Nucl. Phys. Proc. Suppl. 162.